# Unveiling ecological assembly rules from commonalities in trait distributions

Nicolas Gross, Yoann Le Bagousse-Pinguet, Pierre Liancourt, Hugo Saiz,
Cyrille Violle, François Munoz

# Unveiling ecological assembly rules from trait distributions

| | |
|---|---|
| Journal: | *Ecology Letters* |
| Manuscript ID | ELE-01217-2020.R1 |
| Manuscript Type: | Letters |
| Date Submitted by the Author: | 14-Feb-2021 |
| Complete List of Authors: | Gross, Nicolas; INRAE, ECODIV<br>Pinguet, Yoann<br>Liancourt, Pierre; Czech Academy of Sciences, institute of botany; University of Tubingen Faculty of Science,  Plant Ecology Group<br>Saiz, Hugo<br>Violle, Cyrille; CNRS, CEFE<br>Munoz, François; Université Grenoble Alpes, Laboratoire d'Ecologie Alpine |
| | |

1 **Letters**

2 **Running head** Trait diversity and assembly rules

3

4 **Title:** Unveiling ecological assembly rules from trait distributions

5

6 Nicolas Gross[1,†,*], Yoann Le Bagousse-Pinguet[2,*], Pierre Liancourt[3,4,*], Hugo Saiz[5], Cyrille

7 Violle[6], François Munoz[7]

8

9 [1] Université Clermont Auvergne, INRAE, VetAgro Sup, UMR Ecosystème Prairial, 63000

10 Clermont-Ferrand, France.

11 [2] Aix Marseille Univ, CNRS, Avignon Université, IRD, IMBE, Technopôle Arbois-

12 Méditerranée Bât. Villemin – BP 80, F-13545 Aix-en-Provence cedex 04, France.

13 [3] Institute of Botany of the Czech Academy of Science, Průhonice, Czech Republic

14 [4] Plant Ecology Group, University of Tübingen, Tübingen, Germany

15 [5] Institute of Plant Sciences, University of Bern. Altenbergrain 21, 3013 Bern, Switzerland.

16 [6] Centre d'Écologie Fonctionnelle et Évolutive UMR 5175, Univ Montpellier – CNRS – EPHE

17 - IRD –Univ Paul Valéry Montpellier, 1919 route de Mende, 34293 Montpellier Cedex 5,

18 France

19 [7] Univ. Grenoble Alpes, LIPHY, F-38000 Grenoble, France

20

21 † Corresponding Author: nicolas.gross@inrae.fr

22

23 *these authors can be considered as co-first authors

24

25

**Author contributions**

NG, YLB-P. and PL developed the original idea. FM developed the model and the coding. NG

ran the simulations. All co-authors contributed to data interpretation. NG and YLB-P wrote the

first draft of the paper with major contribution from all co-authors.

**Data accessibility statement:** This paper is based on simulations. The authors provide the R

code to generate the simulations with the submitted manuscript. The R code will be archived in

an appropriate public repository with the acceptance of the paper.

**Word count:**

Abstract: 149 words

Main Text: 4566 words

Box 1: 657 words

Number of references: 50

Number of Figures: 5

Number of Box: 1 text box

43 **ABSTRACT**

44 Deciphering the effect of neutral and deterministic processes on community assembly is critical

45 to understand and predict diversity patterns. The information held in community trait

46 distributions is commonly assumed as a signature of these processes, but empirical and

47 modelling attempts have most often failed to untangle their confounding, sometimes opposing,

48 impacts. Here, we simulated the assembly of trait distributions through stochastic (dispersal

49 limitation) and/or deterministic scenarios (environmental filtering, niche differentiation). We

50 characterized the shape of trait distributions through the skewness-kurtosis relationship. We

51 identified commonalities in the co-variation between the skewness and the kurtosis of trait

52 distributions with a unique signature for each simulated assembly scenario. Our findings were

53 robust to variation in the composition of regional species pools, dispersal limitation, and

54 environmental conditions. While ecological communities can exhibit a high degree of

55 idiosyncrasy, identification of commonalities across multiple communities can help to unveil

56 ecological assembly rules in real-world ecosystems.

57

58 **Key words:** dispersal limitation, community assembly rules, environmental filtering,

59 functional diversity, niche differentiation, skewness-kurtosis relationship, stochasticity, trait

60 distributions

**INTRODUCTION**

A basic tenet in community ecology is that trait diversity can reveal the influence of deterministic processes on species assemblages (e.g., competition and abiotic factors; McGill *et al.* 2006; Weiher *et al.* 2011). Central to this research agenda is the hypothesis that high trait diversity reflects niche differentiation processes, while low trait diversity reflects the effect of environmental filtering selecting for species with similar trait values (Cornwell & Ackerly 2009; Maire *et al.* 2012; Keddy 1992; Grime 2006). Much research has been devoted to analyze how patterns of trait diversity vary within and among communities (e.g., convergence or divergence) with the aim to uncover general assembly rules that could apply across many ecosystems (Diamond 1975; Weiher & Keddy 2001). However, hypothesizing a direct and unequivocal linkage between patterns of trait diversity and assembly processes has proved too simplistic and fed much debate (Weiher *et al.* 2011; Götzenberger *et al.* 2012; Münkemüller *et al.* 2020).

Multiple assembly processes are likely to simultaneously influence local trait diversity, sometimes in opposite directions (Mayfield & Levine 2010; Maire *et al.* 2012), making trait diversity patterns often difficult to distinguish from randomness (Götzenberger *et al.* 2012; Munoz & Huneman 2016). The signature of deterministic processes can be blurred by stochastic processes such as demographic drift, or contingent variation in the regional species pool composition (Hubbell 2001; Spasojevic *et al.* 2018). Furthermore, most trait-based approaches have ignored the effect of species dispersal among communities (Spasojevic *et al.* 2014). Dispersal limitation can strongly reduce species richness (Ricklefs 1987), increasing the imprint of local demographic stochasticity (Leibold *et al.* 2004), and thereby yielding apparent randomness in community-level patterns (Götzenberger *et al.* 2012; Munoz & Huneman 2016). Deciphering how multiple stochastic and deterministic processes shape trait diversity is not only crucial to expand our fundamental understanding of biodiversity patterns, but also to better predict the response of communities and ecosystems to ongoing environmental changes.

87    Trait diversity is usually assessed using synthetic indices derived from the distribution

88    of trait values within communities (e.g., Mason *et al.* 2005; Laliberté & Legendre 2010; Enquist

89    *et al.* 2015; Carmona *et al.* 2016). Most studies focus on the mean and variance/dispersion of

90    trait distributions (Violle *et al.* 2012), or on related indices (e.g., FDis, Laliberté & Legendre

91    2010). Considering that mean and variance suffice for describing trait diversity relies on the

92    implicit assumption that trait values follow (approximately) a normal distribution. In essence,

93    the normal distribution shows a bell shape, whose mean represents a local optimum that

94    matches a given environment and the variance represents how trait values are constrained

95    around this mean (Enquist *et al.* 2015, Fig. 1a). However, trait distributions often deviate from

96    a normal distribution in real-world communities, and can exhibit asymmetric, flat, peaky or

97    multimodal shapes (Fig. 1b) (Enquist *et al.* 2017; Le Bagousse-Pinguet *et al.* 2017). In such

98    cases, further information on the shape of trait distributions is required to characterize trait

99    diversity.

100    The shape of trait distributions can be quantified by the skewness and the kurtosis, which

101    quantify the asymmetry and the evenness of the trait distributions, respectively. The skewness

102    and the kurtosis are increasingly used in ecological research because they can provide insights

103    on how species assemble within communities, and how they respond to ongoing environmental

104    changes (Kraft *et al.* 2008; Enquist *et al.* 2015; Gross *et al.* 2017; Wieczynski *et al.* 2019). For

105    instance, rapid environmental changes can simultaneously increase the skewness and kurtosis

106    of trait distributions when a limited portion of the community with specific trait values benefit

107    from the environmental change, and the recruitment of new species adapted to novel conditions

108    is not immediate (see predictions in "Trait Driver Theory" in Enquist *et al.* 2015, 2017).

109    Conversely, niche differentiation should decrease the kurtosis of trait distributions, yielding

110    flatter or even bimodal distributions by promoting the coexistence of functionally contrasting

111    species (Cornwell & Ackerly 2009; Maire *et al.* 2012) .

112    The skewness and the kurtosis are mathematically constrained through the Skewness-

113    Kurtosis Relationship (SKR hereafter), which can be used to characterize a broad spectrum of

114    distributions (Box 1) (Cullen & Frey 1999). Across a variety of dryland plant communities,

115    Gross et al. (2017) reported that the distributions of plant height and specific leaf area followed

116    non-random SKRs. These empirical SKRs suggested the existence of general assembly rules

117    observable at the biome scale where traits organized according to specific families of trait

118    distributions (see Box 1 and Fig. 1c;d for a definition of family of trait distributions). Yet, we

119    do not know which ecological processes underpin such empirical assembly rules, how different

120    deterministic and stochastic processes modulate SKR patterns, and whether the signature of

121    these processes are distinguishable from one another. A theoretical evaluation of the SKR

122    framework is therefore needed to assess the effects of multiple stochastic and deterministic

123    assembly processes on trait distributions, and more generally, to advance our ability to identify

124    assembly rules from patterns of trait distributions.

125    In a theoretical experiment, we simulated the effects of multiple stochastic and

126    deterministic processes on trait diversity patterns. Using the *ecolottery* package in R language

127    (Munoz *et al.* 2018), we generated 800,000 communities spanning a broad spectrum of

128    ecological processes and of resulting trait distributions. Specifically, we considered four

129    community assembly scenarios: (i) a purely neutral scenario including stochastic processes

130    only; and (ii) three different "trait-based" scenarios, each combining stochastic processes with

131    a distinct outcome of deterministic processes entailing either convergence or divergence in trait

132    distributions (Loranger *et al.* 2018). Our goals were:

133    (1) to assess the extent to which the SKR and standard metrics of trait diversity capture

134    distinguishable signatures of assembly processes;

135    (2) to evaluate how the importance of stochastic processes (through the manipulation of

136    the regional species pool richness, and dispersal limitation among communities) and

137     environmental variations across communities affect our ability to identify unambiguous

138     signatures of the four community assembly scenarios.

139

140     **METHODS**

141     **Community assembly scenarios**

142     *ecolottery* is a modeling platform simulating the assembly of ecological communities (Munoz

143     *et al.* 2018). It relies on a spatially implicit framework in which communities are assembled

144     from an external pool of potential immigrants (e.g., a regional species pool) through dispersal.

145     Stochastic and deterministic processes can be parameterized in *ecolottery*. They both influence

146     the establishment success of immigrants and survival of their descendants in the model

147     (Loranger *et al.* 2018; Munoz *et al.* 2018). Stochastic processes influence local diversity

148     through demographic drift, dispersal limitation, and species richness in the regional pool

149     (Etienne & Alonso 2005). Deterministic processes modulate the success of immigrants based

150     on how their trait values allow establishment and persistence in local environments.

151        We simulated three different outcomes of deterministic processes in *ecolottery*

152     henceforth "trait-based filtering". The first trait-based filtering operates around a single optimal

153     value defined by its matching with the local environmental conditions ("stabilizing filtering"

154     hereafter), consistently with the classical view of the environmental filtering (Keddy 1992;

155     Kraft *et al.* 2015). Stabilizing filtering typically generates normal or more leptokurtic

156     distributions (e.g. hyperbolic distributions, Fig. 1 a,b), depending on the strength of the filtering

157     (Enquist *et al.* 2015; Le Bagousse-Pinguet *et al.* 2017). The second trait-based filtering

158     generates assemblages where alternative optimal trait values can confer greater species

159     performance ("disruptive filtering"; Rolhauser & Pucheta 2017; Loranger *et al.* 2018). This

160     trait-based filtering produces patterns that reflect either niche differentiation among

161     functionally contrasting species (Cornwell & Ackerly 2009; Maire *et al.* 2012; Rolhauser &

162    Pucheta 2017). Disruptive filtering typically produces uniform or bimodal distributions (Fig.

163    1b). Finally, the third trait-based filtering generates assemblages in which species performance

164    varies monotonically with trait values ("Directional filtering"). This produces asymmetric trait

165    distributions (Loranger *et al.* 2018) (e.g. exponential distribution in Fig. 1b), e.g. in the case of

166    asymmetric light competition (Schamp *et al.* 2007) or directional environmental changes

167    (Enquist *et al.* 2015).

168

169    **In silico assembly experiment**

170    We considered four theoretical scenarios to assemble communities: (i) a purely neutral scenario

171    that only considers the effect of stochastic processes on assembly without influence of trait

172    differences on species performance and on trait distribution in assemblages (Hubbell 2001);

173    and (ii) three contrasting scenarios in which deterministic processes (aforementioned trait-

174    based filtering) are combined with stochastic processes. We modeled the four scenarios using

175    different values of the parameter "*filt*" in *ecolottery* to represent the "neutral", "stabilizing",

176    "disruptive" and "directional" scenarios (see R code in Appendix S1 in Supporting

177    Information). In addition, we draw species trait values *i* between -3 to +3.

178         In a first simulation experiment, we simulated all communities with the same

179    environmental conditions ("fixed environment", hereafter), under low or high dispersal

180    limitation. Dispersal limitation was manipulated using a migration parameter "*m*" that was set

181    to either low ($m = 0.95$) or high dispersal limitation ($m = 0.05$). In a second simulation

182    experiment, we simulated communities along an environmental gradient. The environmental

183    gradient was simulated by adjusting the parameter "*Env*" from -2 to + 2, corresponding to the

184    two extremes of a gradient (e.g., from cold to hot environments), and where 0 represented the

185    mild environment (see Table S1 for model parameters). We chose the range of environmental

186    variation "*Env*" (ranging from -2 to + 2) to be lower than the range of possible trait values

187    (ranging from -3 to +3) to avoid edge effects (Denelle *et al.* 2019). We set "*m*" to either low or

188    high dispersal limitation as explained in the first simulation experiment.

189         The total number of individuals in the external species pool was set to 25,000. This pool

190    delineates the 'regional species pool' in our simulations. To evaluate how the richness of the

191    species pool influenced community assembly, the pool of immigrants varied from 10 to 500

192    species. Richness at the regional level was fixed for each simulation run. The total number of

193    individuals per community was set to 250 (Table S1), and we simulated 100 communities in

194    each run. We chose these parameter values to approximate "realistic" vegetation sampling in

195    the context of dryland (Gross et al. 2017, Table S1). Within communities, the number of

196    individuals per species could vary according to the simulated assembly processes. The trait

197    values of the regional species pool followed a uniform distribution, such that all trait values had

198    equal probability of being selected. We randomly assigned trait values to each species. During

199    this procedure, the model allowed different species to exhibit similar trait values, therefore

200    allowing functional redundancy to occur among species (Munoz *et al.* 2018). For simplicity,

201    we did not consider intraspecific trait variability in our simulations. Conspecific individuals

202    thus displayed the same trait value.

203

**Analysis of simulated trait distributions**

205    We generated 800,000 communities: 500 runs where species richness varied from 10 to 500

206    species in the species pool × 100 communities per run × 4 scenarios × 2 levels of dispersal

207    limitation (low vs. high) × 2 environmental contexts (a fixed environment vs. an environmental

208    gradient). For each run, we recorded the total number of species in a given community (species

209    richness). We quantified species relative abundance as the relative frequency of each species in

210    each community (i.e., the number of individual of a species divided by the total number of

211    individual in the community).

212        We calculated the four moments of the trait distribution associated to each simulated

213    community: the mean, variance, skewness and kurtosis. Then, we calculated the parameters of

214    the SKRs across the 100 simulated distributions obtained from each run (R², slope, Y-intercept

215    and the distance to the lower boundary; see Box 1). For each community, we also computed

216    classical indices of trait diversity using the dbFD function in the "FD" package in R [functional

217    dispersion (FDis), the Rao index, functional evenness (FEve); Laliberté and Legendre 2010].

218    The four distribution moments and all trait diversity metrics were abundance-weighted. While

219    the SKR parameters were estimated across the 100 communities generated by each simulation

220    run, the four distribution moments, and taxonomic and trait diversity indices were calculated at

221    the community level, and thus generated 100 values for each run.

222        We evaluated whether the parameters of the SKRs, the four distribution moments and

223    all diversity metrics can be used to discriminate assembly processes from trait distributions. For

224    instance, lower variance, FDis and Rao values compared to the neutral scenario are expected

225    for the stabilizing and directional filtering, i.e., trait convergence. Conversely, higher variance,

226    FDis and Rao values compared to the neutral scenario are expected for the disruptive filtering,

227    i.e., trait divergence. To test for significant differences among scenarios, we used the "overlap"

228    package in R (Ridout & Linkie 2009). For each diversity metric, we calculated the overlap

229    between each pair of scenarios and the mean overlap considering all scenarios together. Overlap

230    values ranged from 0 to 1. An overlap < 0.05 indicated that the metric under consideration

231    significantly discriminate assembly scenarios.

232

233    **RESULTS**

234    **Discriminating scenarios using functional diversity metrics**

235    The neutral scenario generated a wide range of trait diversity patterns, which challenges the

236    inference of ecological processes from trait distributions (Figs. 2, 3). Significant differences

237     among scenarios were observed under low dispersal limitation. For instance, we observed

238     significant differences between the stabilizing and the neutral scenarios for FDis and for Rao

239     under low dispersal limitation (Figs. 2, 3). However, under high dispersal limitation, all trait

240     diversity indices - with the exception of the variance - simulated under the neutral scenario

241     systematically overlapped with those of the deterministic scenarios, meaning a lack of

242     differences among them.

243          The variance of trait distributions best discriminated assembly scenarios. We observed

244     a low mean overlap (Mo) when dispersal limitation was low and under fixed environment (Mo

245     = 0.01, Fig. 2a, left panel). The stabilizing and directional scenarios exhibited significantly

246     lower variances than those of the neutral scenario. However, the variance could not discriminate

247     the stabilizing from the disruptive and directional scenarios, and the neutral from the disruptive

248     scenario along an environmental gradient combined with high dispersal limitation (Mo = 0.16,

249     Fig. 2b). Overall, our results showed limited ability of these metrics of trait diversity to identify

250     unambiguous signatures of the four community assembly scenarios.

251

252     **SKR parameters simulated in a fixed environment**

253     Each studied scenario generated contrasting SKR patterns under fixed environmental

254     conditions and low dispersal limitation (Fig. 4, see also SKR plots in Fig. S1). The neutral and

255     stabilizing scenarios both generated weaker SKRs than the disruptive and directional scenarios

256     (significantly lower $R^2$, Fig. 4b). These first two scenarios produced distributions that clustered

257     in the skewness-kurtosis space, and tended to overall converge toward a single skewness-

258     kurtosis coordinate as species richness in the regional pool increased (from dark to bright blue

259     dots, Fig. 4a). In contrast, both the directional and the disruptive scenarios yielded strong SKRs,

260     i.e. characterized by significantly higher $R^2$ than neutral and stabilizing scenarios (Fig. 4b).

261     Specifically, the disruptive scenario generated SKRs with the highest $R^2$, ranging from 0.6 to

262  0.99 (Fig. 4b), indicating that all communities assembled under this scenario belong to a unique

263  family of trait distributions (skew-bimodal distribution, Fig. 1c, d).

264      The SKRs generated from the four scenarios had also clear and significantly distinct Y-

265  intercepts (Fig. 4b). Therefore, the SKR not only discriminated the three scenarios containing

266  deterministic processes from a purely neutral scenario, but also clearly differentiated these three

267  scenarios from one another. The neutral scenario had a Y-intercept = 1.86 (Fig. 4b) suggesting

268  that it converged toward uniform distribution (Fig. 1b). This pattern of trait diversity observed

269  at the Y-intercept of the SKR thus mirrored the trait distribution of the regional pool. The

270  stabilizing scenario produced communities that converged toward a normal distribution (Y-

271  intercept = 2.82 Fig. 4b). This scenario generated a peakier and therefore less even trait

272  distribution than the neutral one. The directional scenario generated distributions that were

273  mostly asymmetric, and that converged toward a skewness value ~1 as species richness

274  increased (Fig. 4a) and a Y-intercept = 2.1 (Fig. 4b). The disruptive scenario had the lowest Y-

275  intercept = 1.33 (Fig. 4b). This scenario generated a family of trait distributions approaching

276  the lower boundary of the skewness-kurtosis space, corresponding to highly platykurtic

277  bimodal distributions (see the skew-bimodal distribution in Fig. 1c). Therefore, the disruptive

278  scenario was the one with the highest trait diversity in our simulations.

279      Increasing the influence of stochasticity, through high dispersal limitation, reduced the

280  species richness at the community level (Fig. S2). It consistently increased the asymmetry of

281  trait distributions for all scenarios, thereby increasing the scatter of distributions in the

282  skewness-kurtosis space (Fig. 4a). Higher scattering of skewness and kurtosis values produced

283  SKRs with higher $R^2$ for all scenarios (Fig. 4b). For instance, the $R^2$ of the neutral scenario

284  ranged from 0.25 to 0.75 (Fig. 4b), indicating that significant SKRs can be observed and

285  produced by a high stochasticity even under a strictly neutral scenario. Yet, irrespective of the

286  degree of stochasticity, the disruptive filtering always produced the strongest SKRs (Fig. 4b).

287    Furthermore, increasing dispersal limitation marginally influenced the Y-intercept of the SKRs.

288    The mean overlap among scenarios remained extremely low under high dispersal limitation (Y-

289    intercept: $Mo = 0.03$, Fig. 4b). We observed significant differences between the stabilizing,

290    neutral and disruptive scenarios, although the directional scenario overlapped with the neutral

291    one (overlap $= 0.18$). These results suggested that the SKR approach is therefore able to

292    differentiate a neutral assembly scenario from the effect of environmental filtering (stabilizing

293    scenario) and niche differentiation (disruptive scenario) even under a high stochasticity.

294

295    **SKR parameters simulated along an environmental gradient**

296    Changing environmental conditions across communities affected local mean trait value for all

297    the studied scenarios except the neutral one (Fig. S3). Furthermore, the variance was constant

298    and low for the stabilizing scenario while all moments varied under the disruptive scenario (Fig.

299    S3). For the disruptive scenario, increasing the environmental constraint (by changing the *Env*

300    parameter from 0 to -2 or from 0 to +2) reduced the variance and increased the skewness and

301    the kurtosis (Fig. S3a). Nevertheless, the SKR parameters calculated across communities along

302    the gradient, and particularly the Y-intercept, consistently produced similar patterns than those

303    observed under a fixed environment with significant differences among scenarios (Y-intercept

304    $Mo = 0.005$ with low dispersal limitation, Y-intercept $Mo = 0.04$ with high dispersal limitation

305    Fig. 5b). The $R^2$ of the SKRs also differed among scenarios with the stabilizing scenario

306    showing the lowest range of $R^2$ and the disruptive scenario showing the highest $R^2$ (Fig. 5b).

307

308    **DISCUSSION**

309    **Commonalities in trait distributions across multiple communities unveil assembly rules**

310    Our reference neutral scenario generated a wide range of trait diversity patterns, following the

311    view that "*simple stochastic models can reproduce natural diversity patterns*" (Hubbell 2005).

312 Likewise, deterministic assembly scenarios generated a wide range of trait distributions

313 (Enquist *et al.* 2015; Le Bagousse-Pinguet *et al.* 2017). The ambiguity among scenarios further

314 increased in our simulations as stochasticity increased or when the environmental conditions

315 changed (e.g., sampling performed along environmental gradients). Therefore, our study

316 therefore demonstrates that distinguishing deterministic from purely neutral patterns based on

317 standard trait-based metrics, or by the four moments of trait distributions taken separately, is

318 particularly challenging.

319       The SKR framework provided far less ambiguous insights into underlying assembly

320 processes, as contrasting assembly scenarios exhibited distinct SKR patterns. The SKR

321 approach did not only well discriminate the neutral from trait-based filtering scenarios, but also

322 clearly differentiated each of the filtering scenarios from one another, irrespective of the degree

323 of dispersal limitation, environmental condition or the size of the species pool. The SKR

324 approach appears therefore as a promising tool to unveil assembly processes from trait

325 distributions, even under high stochasticity, a yet important limitation of existing approaches

326 aiming at interpreting trait diversity patterns of real-world communities (Weiher *et al.* 2011;

327 Münkemüller *et al.* 2020).

328       The SKR framework shifts our perspective to focus on commonalities in trait

329 distributions - rather than differences – to unveil assembly rules. For instance, the disruptive

330 filtering generated a set of symmetric and asymmetric distributions. Under this scenario,

331 increasing environmental constraints simultaneously reduced the variance and increased both

332 the skewness and the kurtosis of trait distributions (Enquist *et al.* 2015; Le Bagousse-Pinguet

333 *et al.* 2017), consistently with the environmental filtering hypothesis (Keddy 1992). However,

334 the trait distributions all aligned along a specific SKR. The observed SKR pattern thus described

335 a family of trait distributions, in which each single distribution represents an instance of a more

336 general trait distribution operating at larger spatial scale (e.g., at the biome scale in Gross *et al.*

337   2017). All distributions within this family shared a common property: trait distributions are

338   bimodal (Fig. S5), thus reflecting the effect of niche differentiation processes promoting the

339   coexistence of functionally contrasting species (Maire *et al.* 2012). In other words, even if

340   different environmental conditions along a gradient (and stochastic processes) can affect the

341   shape parameters of distributions by increasing the skewness and the kurtosis separately, a

342   bimodality persists as the signature of niche differentiation. By characterizing commonalities

343   in trait distributions, the SKR represents a critical step toward the identification of general rules

344   governing the functional organization of species assemblages.

345          By identifying families of trait distributions, the SKR framework scales up trait

346   distributions from the community to broader geographical scales (e.g. landscape / regional /

347   continental / biome scales). The SKR framework differs from other trait-based approaches

348   aiming at addressing biogeographical questions by aggregating trait patterns across spatial

349   scales (Violle *et al.* 2014; Carmona *et al.* 2016). While the SKR framework scales up trait

350   distributions from local to wider geographical scales, it also keeps the information on the shape

351   of trait distributions observed at the community scale. In other words, the SKR framework

352   increases the spatial extent by quantifying trait distributions at large spatial scale but does not

353   reduce the grain size. Therefore, the SKR framework represents an opportunity to merge

354   community ecology and biogeography and to "*achieve a deeper understanding of biodiversity*

355   *and its change across communities*" (Chase *et al.* 2018).

356          The skewness and the kurtosis of trait distributions are increasingly used to detect the

357   short term effects of global change on communities, and may be used as a signal of

358   compositional changes (Enquist *et al.* 2017; Griffin-Nolan *et al.* 2019; Wieczynski *et al.* 2019;

359   Zhang *et al.* 2019; Aguirre-Gutiérrez *et al.* 2020). Yet, variations in skewness and kurtosis are

360   often considered independently, i.e. without accounting for their mathematical dependency

361   (Box 1). Observing a decrease in trait evenness (higher kurtosis) may entirely rely on changes

362   in the degree of skewness. Accounting for the SKR when assessing the impact of global change

363   on ecological communities should provide additional insights on how the ecological reassembly

364   under environmental change, and may provide a more robust validation of theoretical

365   predictions (e.g. the "Trait Driver Theory": Enquist et al. 2015, 2017). Focusing on the distance

366   to the lower boundary of the SKR (see Box 1) (Liu *et al.* 2020) or the deviation of individual

367   communities from empirical to random SKR (Gross *et al.* 2017) – rather than raw variations in

368   kurtosis - may help diagnosing shifts in community evenness and community disassembly

369   under ongoing environmental change.

370

371   **Linking theoretical predictions to empirical patterns of trait diversity**

372   Our simulations suggest that niche differentiation and dispersal limitation jointly shape the trait

373   diversity in real-world communities. Combining the disruptive scenario with high dispersal

374   limitation was the only case that generated a strong family of trait distributions (i.e., a SKR

375   with a $R^2 > 0.90$). This family of trait distributions exhibited lower kurtosis than under the

376   neutral scenario, a pattern similar to the empirical SKRs observed in drylands worldwide (Gross

377   et al. 2017). When simulating along an environmental gradient, the disruptive scenario also

378   reproduced the impact of environmental filtering by reducing variance and increasing the

379   kurtosis within communities (Fig. S3), and the shift in dominance of contrasting functional

380   groups (e.g. the shrub-to-grass shift in dominance commonly observed in drylands; Fig. S4,

381   Bestelmeyer *et al.* 2018). Altogether, our results corroborate the view that dryland communities

382   are shaped by a combination of these multiple drivers.

383        The modelling platform *ecolottery* provides a simple and flexible environment to

384   simulate the effect of multiple stochastic and deterministic processes on trait distributions

385   (Munoz *et al.* 2018). Further implementations are needed to provide reliable and quantitative

386    predictions when comparing theoretical predictions with observed trait distributions in real-

387    world communities:

388          First, different assembly processes have been shown to act differently on traits

389    describing contrasted axes of functional specialization (e.g. size vs. resource use related-traits,

390    Kraft *et al.* 2008; Cornwell & Ackerly 2009; Maire *et al.* 2012). On the one hand, the disruptive

391    scenario may well apply to resource-use traits as contrasting strategies for resources acquisition

392    and utilization may favor species coexistence (Maire *et al.* 2012). On the other hand, the

393    directional scenario could constitute a valuable hypothesis for size-related traits in light limited

394    environments where asymmetric competition predominates (Schamp *et al.* 2007; Gross *et al.*

395    2009). Considering the effect of multiple assembly processes acting on independent functional

396    dimensions would allow a more realistic representation of community assembly and species

397    coexistence (Maire *et al.* 2012).

398          Second, the distributions of trait values at large spatial scale (e.g. at the scale of the

399    regional species pool) are important drivers determining local assembly processes and trait

400    diversity (Carmona *et al.* 2016; Le Provost *et al.* 2017; Spasojevic *et al.* 2018). To evaluate

401    how regional trait pools influence SKR patterns, we conducted a sensitivity analysis using

402    different trait distributions at the regional scale (see Fig. S5 for details). Our results show that

403    the regional trait pool influenced the SKR parameters for each scenario. It supports the need to

404    account for the regional trait pool to provide reliable predictions on trait diversity within and

405    across communities (Carmona *et al.* 2016; Spasojevic *et al.* 2018). Nevertheless, we also

406    observed that the relative differences among contrasting assembly scenarios remained

407    consistent despite variation in the composition of the regional trait pool, highlighting the

408    robustness of the SKR approach.

409          Third, downscaling from a global / regional trait pool to the local community scale may

410    require the development of a spatially-explicit framework, as contrasting assembly processes

17

411  may act simultaneously but at different spatial scale (Keddy 1992; Spasojevic *et al.* 2014; Le

412  Provost *et al.* 2017). Such framework would allow evaluating how environmental filtering

413  acting at broad spatial scale (Kraft *et al.* 2015; Le Bagousse-Pinguet *et al.* 2017) interacts with

414  local biotic processes (Maire *et al.* 2012), e.g. by simulating the stabilizing and disruptive

415  scenarios within a single framework but acting at contrasted spatial scale. In this context, further

416  implementations of the model would allow for a more explicit representation of biotic

417  interactions. For instance, the disruptive scenario considers a selection of two optima due to

418  alternative suitable strategies (e.g., coexisting guilds, Cornwell & Ackerly 2009; Maire *et al.*

419  2012). However, the disruptive scenario does not account for interactions among individual

420  species trough density-dependent mechanisms (MacArthur & Levins 1967) as well as for other

421  types of biotic interactions (e.g., facilitation and indirect interactions) that have been shown to

422  impact trait diversity in plant communities (Gross *et al.* 2009; Saiz *et al.* 2019).

423

424  **Conclusions**

425  Here we show that the skewness-kurtosis relationship (SKR) offers a powerful mean to evaluate

426  the effect of multiple stochastic and deterministic processes on the assembly of ecological

427  communities. By focusing on the co-variation between the skewness and the kurtosis across

428  multiple communities, the SKR framework identifies commonalities in the shape of the trait

429  distributions that can serve as a basis to infer assembly processes. The SKR framework is robust

430  to stochastic processes such as variation in regional species and trait pools, dispersal limitation.

431  Finally, our simulations suggest that the joint effect of local-scale processes such as niche

432  differentiation and regional-scale dispersal limitation can have key implications for shaping

433  biodiversity. Our study offers promising avenue for identifying ecological assembly rules in

434  real-world ecosystems.

435

**Acknowledgments**

**REFERENCES**

Aguirre-Gutiérrez, J., Malhi, Y., Lewis, S.L., Fauset, S., Adu-Bredu, S., Affum-Baffoe, K., *et al.* (2020). Long-term droughts may drive drier tropical forests towards increased functional, taxonomic and phylogenetic homogeneity. *Nature communications*, 11, 1–10.

Bestelmeyer, B.T., Peters, D.P.C., Archer, S.R., Browning, D.M., Okin, G.S., Schooley, R.L., *et al.* (2018). The Grassland–Shrubland Regime Shift in the Southwestern United States: Misconceptions and Their Implications for Management. *BioScience*, 68, 678–690.

461   Carmona, C.P., de Bello, F., Mason, N.W.H. & Lepš, J. (2016). Traits Without Borders:

462   Integrating Functional Diversity Across Scales. *Trends in Ecology & Evolution*, 31,

463   382–394.

464   Chase, J.M., McGill, B.J., McGlinn, D.J., May, F., Blowes, S.A., Xiao, X., *et al.* (2018).

465   Embracing scale-dependence to achieve a deeper understanding of biodiversity and its

466   change across communities. *Ecology Letters*, 21, 1737–1751.

467   Cornwell, W.K. & Ackerly, D.D. (2009). Community assembly and shifts in plant trait

468   distributions across an environmental gradient in coastal California. *Ecological*

469   *Monographs*, 79, 109–126.

470   Cristelli, M., Zaccaria, A. & Pietronero, L. (2012). Universal relation between skewness and

471   kurtosis in complex dynamics. *Phys. Rev. E*, 85, 066108.

472   Cullen, A.C., Frey, H.C. & Frey, C.H. (1999). *Probabilistic techniques in exposure*

473   *assessment: a handbook for dealing with variability and uncertainty in models and*

474   *inputs*. Springer Science & Business Media.

475   Denelle, P., Violle, C. & Munoz, F. (2019). Distinguishing the signatures of local

476   environmental filtering and regional trait range limits in the study of trait–environment

477   relationships. *Oikos*, 128, 960–971.

478   Diamond, J.M. (1975). The island dilemma: lessons of modern biogeographic studies for the

479   design of natural reserves. *Biological conservation*, 7, 129–146.

480   Enquist, B.J., Bentley, L.P., Shenkin, A., Maitner, B., Savage, V., Michaletz, S., *et al.* (2017).

481   Assessing trait-based scaling theory in tropical forests spanning a broad temperature

482   gradient. *Global Ecology and Biogeography*, 26, 1357–1373.

483   Enquist, B.J., Norberg, J., Bonser, S.P., Violle, C., Webb, C.T., Henderson, A., *et al.* (2015).

484   Chapter Nine - Scaling from Traits to Ecosystems: Developing a General Trait Driver

485   Theory via Integrating Trait-Based and Metabolic Scaling Theories. In: *Advances in*

486    *Ecological Research*, Trait-Based Ecology - From Structure to Function (eds. Pawar,

487    S., Woodward, G. & Dell, A.I.). Academic Press, pp. 249–318.

488    Etienne, R.S. & Alonso, D. (2005). A dispersal-limited sampling theory for species and

489    alleles: A dispersal-limited sampling theory. *Ecology Letters*, 8, 1147–1156.

490    Götzenberger, L., de Bello, F., Br\aathen, K.A., Davison, J., Dubuis, A., Guisan, A., *et al.*

491    (2012). Ecological assembly rules in plant communities—approaches, patterns and

492    prospects. *Biological reviews*, 87, 111–127.

493    Griffin-Nolan, R.J., Blumenthal, D.M., Collins, S.L., Farkas, T.E., Hoffman, A.M., Mueller,

494    K.E., *et al.* (2019). Shifts in plant functional composition following long-term drought

495    in grasslands. *Journal of Ecology*, 107, 2133–2148.

496    Grime, J.P. (2006). Trait convergence and trait divergence in herbaceous plant communities:

497    mechanisms and consequences. *Journal of Vegetation Science*, 17, 255–260.

498    Gross, N., Kunstler, G., Liancourt, P., Bello, F.D., Suding, K.N. & Lavorel, S. (2009).

499    Linking individual response to biotic interactions with community structure: a trait-

500    based framework. *Functional Ecology*, 23, 1167–1178.

501    Gross, N., Le Bagousse-Pinguet, Y., Liancourt, P., Berdugo, M., Gotelli, N.J. & Maestre, F.T.

502    (2017). Functional trait diversity maximizes ecosystem multifunctionality. *Nature

503    ecology & evolution*, 1, 0132.

504    Hubbell, S.P. (2001). *The Unified Neutral Theory of Biodiversity and Biogeography (MPB-

505    32)*. Princeton University Press.

506    Hubbell, S.P. (2005). Neutral theory in community ecology and the hypothesis of functional

507    equivalence. *Functional ecology*, 19, 166–172.

508    Keddy, P.A. (1992). Assembly and response rules: two goals for predictive community

509    ecology. *Journal of vegetation science*, 3, 157–164.

510   Kraft, N.J., Adler, P.B., Godoy, O., James, E.C., Fuller, S. & Levine, J.M. (2015).

511        Community assembly, coexistence and the environmental filtering metaphor.

512        *Functional ecology*, 29, 592–599.

513   Kraft, N.J.B., Valencia, R. & Ackerly, D.D. (2008). Functional Traits and Niche-Based Tree

514        Community Assembly in an Amazonian Forest. *Science*, 322, 580–582.

515   Laliberté, E. & Legendre, P. (2010). A distance-based framework for measuring functional

516        diversity from multiple traits. *Ecology*, 91, 299–305.

517   Le Bagousse-Pinguet, Y., Gross, N., Maestre, F.T., Maire, V., de Bello, F., Fonseca, C.R., *et*

518        *al.* (2017). Testing the environmental filtering concept in global drylands. *Journal of*

519        *Ecology*, 105, 1058–1069.

520   Le Provost, G., Gross, N., Börger, L., Deraison, H., Roncoroni, M. & Badenhausser, I. (2017).

521        Trait-matching and mass effect determine the functional response of herbivore

522        communities to land-use intensification. *Funct Ecol*, 31, 1600–1611.

523   Leibold, M.A., Holyoak, M., Mouquet, N., Amarasekare, P., Chase, J.M., Hoopes, M.F., *et al.*

524        (2004). The metacommunity concept: a framework for multi-scale community

525        ecology: The metacommunity concept. *Ecology Letters*, 7, 601–613.

526   Liu, C., Li, Y., Zhang, J., Baird, A.S. & He, N. (2020). Optimal Community Assembly

527        Related to Leaf Economic-Hydraulic-Anatomical Traits. *Frontiers in plant science*,

528        11, 341.

529   Loranger, J., Munoz, F., Shipley, B. & Violle, C. (2018). What makes trait-abundance

530        relationships when both environmental filtering and stochastic neutral dynamics are at

531        play? *Oikos*, 127, 1735–1745.

532   MacArthur, R. & Levins, R. (1967). The limiting similarity, convergence, and divergence of

533        coexisting species. *The american naturalist*, 101, 377–385.

534    Maire, V., Gross, N., Börger, L., Proulx, R., Wirth, C., Pontes, L. da S., *et al.* (2012). Habitat

535        filtering and niche differentiation jointly explain species relative abundance within

536        grassland communities along fertility and disturbance gradients. *New Phytologist*, 196,

537        497–509.

538    Mason, N.W.H., Mouillot, D., Lee, W.G. & Wilson, J.B. (2005). Functional richness,

539        functional evenness and functional divergence: the primary components of functional

540        diversity. *Oikos*, 111, 112–118.

541    Mayfield, M.M. & Levine, J.M. (2010). Opposing effects of competitive exclusion on the

542        phylogenetic structure of communities. *Ecology letters*, 13, 1085–1093.

543    McGill, B.J., Enquist, B.J., Weiher, E. & Westoby, M. (2006). Rebuilding community

544        ecology from functional traits. *Trends in ecology & evolution*, 21, 178–185.

545    Münkemüller, T., Gallien, L., Pollock, L.J., Barros, C., Carboni, M., Chalmandrier, L., *et al.*

546        (2020). Dos and don'ts when inferring assembly rules from diversity patterns. *Global

547        Ecology and Biogeography*.

548    Munoz, F., Grenié, M., Denelle, P., Taudière, A., Laroche, F., Tucker, C., *et al.* (2018).

549        ecolottery: Simulating and assessing community assembly with environmental

550        filtering and neutral dynamics in R. *Methods in Ecology and Evolution*, 9, 693–703.

551    Munoz, F. & Huneman, P. (2016). From the Neutral Theory to a Comprehensive and

552        Multiscale Theory of Ecological Equivalence. *The Quarterly Review of Biology*, 91,

553        321–342.

554    Ricklefs, R.E. (1987). Community diversity: relative roles of local and regional processes.

555        *Science*, 235, 167–171.

556    Ridout, M.S. & Linkie, M. (2009). Estimating overlap of daily activity patterns from camera

557        trap data. *JABES*, 14, 322–337.

558    Rolhauser, A.G. & Pucheta, E. (2017). Directional, stabilizing, and disruptive trait selection

559        as alternative mechanisms for plant community assembly. *Ecology*, 98, 668–677.

560    Saiz, H., Le Bagousse-Pinguet, Y., Gross, N. & Maestre, F.T. (2019). Intransitivity increases

561        plant functional diversity by limiting dominance in drylands worldwide. *Journal of*

562        *Ecology*, 107, 240–252.

563    Schamp, B.S., Chau, J. & Aarssen, L.W. (2007). Dispersion of traits related to competitive

564        ability in an old-field plant community. *J Ecology*, 0, 071119203335008-???

565    Shmida, A. & Ellner, S. (1984). Coexistence of plant species with similar niches. *Vegetatio*,

566        58, 29–55.

567    Spasojevic, M.J., Catano, C.P., LaManna, J.A. & Myers, J.A. (2018). Integrating species traits

568        into species pools. *Ecology*, 99, 1265–1276.

569    Spasojevic, M.J., Copeland, S. & Suding, K.N. (2014). Using functional diversity patterns to

570        explore metacommunity dynamics: a framework for understanding local and regional

571        influences on community structure. *Ecography*, 37, 939–949.

572    Violle, C., Enquist, B.J., McGill, B.J., Jiang, L.I.N., Albert, C.H., Hulshof, C., *et al.* (2012).

573        The return of the variance: intraspecific variability in community ecology. *Trends in*

574        *ecology & evolution*, 27, 244–252.

575    Violle, C., Reich, P.B., Pacala, S.W., Enquist, B.J. & Kattge, J. (2014). The emergence and

576        promise of functional biogeography. *PNAS*, 111, 13690–13696.

577    Weiher, E., Freund, D., Bunton, T., Stefanski, A., Lee, T. & Bentivenga, S. (2011). Advances,

578        challenges and a developing synthesis of ecological community assembly theory.

579        *Philosophical Transactions of the Royal Society B: Biological Sciences*, 366, 2403–

580        2413.

581    Weiher, E. & Keddy, P. (2001). *Ecological assembly rules: perspectives, advances, retreats*.

582        Cambridge University Press.

583 Wieczynski, D.J., Boyle, B., Buzzard, V., Duran, S.M., Henderson, A.N., Hulshof, C.M., *et*

584 *al.* (2019). Climate shapes and shifts functional biodiversity in forests worldwide.

585 *Proceedings of the National Academy of Sciences*, 116, 587–592.

586 Zhang, D., Peng, Y., Li, F., Yang, G., Wang, J., Yu, J., *et al.* (2019). Trait identity and

587 functional diversity co-drive response of ecosystem productivity to nitrogen

588 enrichment. *Journal of Ecology*, 107, 2402–2414.

589

590 **SUPPORTING INFORMATION**

591 Additional Supporting Information may be downloaded via the online version of this article at

592 Wiley Online Library (www.ecologyletters.com).

593 As a service to our authors and readers, this journal provides supporting information supplied

594 by the authors. Such materials are peer-reviewed and may be re-organized for online delivery,

595 but are not copy-edited or typeset. Technical support issues arising from supporting information

596 (other than missing files) should be addressed to the authors.

598    **BOX 1: The Skewness-Kurtosis Relationship (SKR)**

599    We examined whether the relationship between the skewness and the kurtosis of trait

600    distributions (Fig. 1a) can help deciphering the signatures of contrasting assembly processes.

601    The approach is inspired by optimization procedures increasingly used in physics, climatology

602    and economy (e.g. Cristelli *et al.* 2012). We apply the approach to diagnose assembly rules

603    from trait distributions (the Skewness-Kurtosis Relationship [SKR] approach). While the mean

604    and variance reflect the location and the scale of a distribution (the latter being the dispersion

605    of trait values within a community), the skewness and kurtosis inform on its shape. The degree

606    of skewness quantifies the asymmetry of a given distribution. For instance, a skew distribution

607    indicates the dominance of extreme trait values (see exponential distribution in Fig. 1b), which

608    can typically arise from asymmetric competition for light  (Schamp *et al.* 2007). The kurtosis

609    quantifies the relative peakiness of a trait distribution and the relative density of its tails. Low

610    kurtosis values reflect an even distribution of trait values within a given community, a definition

611    of a high trait diversity (Gross et al. 2017). Low Kurtosis may reflect the coexistence of

612    functionally contrasting species (see uniform and bimodal distributions in Fig. 1b) (Enquist *et*

613    *al.* 2017; Gross *et al.* 2017). In contrast, peaked distributions characterized by high kurtosis

614    value reflect a low trait diversity, and may typically occur under strong environmental filtering

615    (sensu Keddy 1992) selecting for a limited range of trait value (see hyperbolic distribution in

616    Fig. 1b).

617        Skewness (S) and kurtosis (K) are related through the following inequality (Fig. 1b):

618                                    $K \geq \beta S^2 + \alpha$                        (1)

619    This inequality generates a mathematically constrained triangle in which all possible trait

620    distributions can be represented and characterized (Gross *et al.* 2017), i.e. the skewness-kurtosis

621    space. For instance, the normal distribution is defined by a unique combination of skewness

622    and kurtosis values of 0 and 3 respectively. It can therefore be represented as a single coordinate

623    in the skewness-kurtosis space (red dot, in Fig. 1d). Families of trait distributions can also be

624    represented by a skewness-kurtosis relationship (SKR, hereafter) with a slope β and a Y-

625    intercept α. A SKR implies that when trait distributions become more skewed, they also become

626    more peaked, resulting in a decrease in evenness. The slope β of the SKR measures the strength

627    of the relationship, i.e., the extent to which evenness decreases as trait distributions become

628    more skewed. The Y-intercept α indicates the lowest kurtosis value at skewness = 0, and

629    corresponds to the highest trait diversity predicted by a given SKR. Distributions belonging to

630    a family of distributions share common properties. For instance, in the case of a skew-bimodal

631    distribution (Fig. 1c, green dashed line in Fig. 1d), all distributions are bimodal although their

632    degree of skewness and kurtosis can vary across communities. This would be the case when

633    two distinct functional groups coexist within communities (e.g. grass and shrub species) but

634    their relative abundance can vary across communities.

635        The inequality (1) has a lower boundary that sets a limit to the minimal kurtosis value

636    predicted for any degree of skewness, i.e. the potential maximum trait diversity for a given

637    skewness (black dash line, $K = S^2 + 1$, Fig. 1b) (see Gross et al. 2017 for a mathematical

638    demonstration). The distance to the lower boundary for a given distribution - exemplified with

639    the black arrow in the case of the exponential distribution (Fig. 1b) - thus quantifies the extent

640    to which trait diversity departs from the potential maximum trait diversity independently from

641    the degree of skewness. Although skewness and kurtosis individually provide valuable

642    information on community trait distributions, the SKR approach helps to diagnose complex

643    trait distributions (Cullen & Frey 1999) and to reveal the extent to which trait diversity is

644    maximized within communities. Applying the SKR framework to ecological communities may

645    allow identifying assembly rules through the identification of commonalities in the shape of the

646    trait distributions observed across multiple communities.

647

648 **Figures Legend:**

649 **Figure 1** Characterizing complex trait distributions using the Skewness-Kurtosis Relationship

650 (SKR). (**a**) A trait distribution is a density function representing the relative frequency or

651 abundance of trait values within a community. Examples of trait distributions include normal

652 (panel a), uniform, bimodal, hyperbolic or exponential distributions (panel b). (c) Example of

653 a family of distributions: a skew-bimodal distribution (see results, and Box 1). (d) The

654 Skewness-Kurtosis space. Trait distributions are characterized by distinct skewness (S) -

655 kurtosis (K) coordinates. Families of trait distributions can be characterized by a specific

656 Skewness-Kurtosis Relationship (SKR) such as $K = \beta S^2 + \alpha$. The distance to the lower boundary

657 (i.e. potential minimum kurtosis value) of a given distribution (exemplified with the black arrow

658 in the case of the exponential distribution) quantifies the extent to which trait evenness is

659 maximized.

660

661 **Figure 2** The four moments of the trait distributions simulated under the four theoretical

662 scenarios (Neutral [Neu], Stabilizing [Sta], Disruptive [Dis], Directional [Dir]) under **(a)** fixed

663 environment and varying species pools, **(b)** changing environment and fixed species pool, and

664 under low / high dispersal limitation. We represent the mean, variance, skewness and kurtosis

665 of the trait distributions simulated under each scenario using violin plots. For each panel, we

666 provide the mean overlap (Mo) among the four moments of the trait distributions. Different

667 letters indicate significant differences between scenarios (overlap < 0.05; NS for Not-
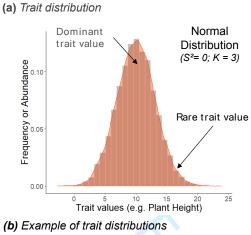
668 Significant).

669

670 **Figure 3** Species richness (Sp. Rich.) and commonly-used trait diversity indices (FDis, Rao,

671 FEve) simulated under the four theoretical scenarios (Neutral [Neu], Stabilizing [Sta],

672 Disruptive [Dis], Directional [Dir]) in **(a)** Fixed environment varying species pools, **(b)**
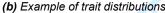
673    changing environment fixed species pool, and under low / high dispersal limitation. We

674    represent each predicted parameter using violin plots. For each panel, we provide the mean

675    overlap (Mo) between the four-parameter distributions. Different letters indicate significant

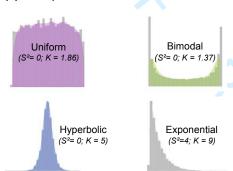676    differences between scenarios (overlap < 0.05; but NS for Not-Significant).

677

678    **Figure 4** Effect of the different assembly scenarios on the Skewness-Kurtosis Relationship

679    (SKR) in a fixed environment and varying regional species pool. **(a)** Coordinates of the

680    simulated communities in the skewness-kurtosis space under the different scenarios. We

681    simulate 100 communities (number of run = 500) assembled in a constant environment under

682    low / high dispersal limitation. Dark and light blue dots represent poor and rich regional pools,

683    respectively. **(b)** We represent the parameters of the SKRs ($R^2$, Y-intercept (alpha), slope of the

684    SKRs (beta), distance to the lower boundary) for each scenario using violin plots. We provide

685    the mean overlap (Mo) among the four scenarios. Different letters indicate significant

686    differences between scenarios (overlap < 0.05; but NS for Not-Significant).

687

688    **Figure 5** Effect of the different assembly scenarios on the Skewness-Kurtosis Relationship

689    (SKR) along an environmental gradient. **(a)** Coordinates of the simulated communities in the

690    skewness-kurtosis space under the different scenarios. We simulated 100 communities (number

691    of run = 500) assembled along an environmental gradient (from Env = -2 to Env = +2) and a

692    fixed regional species pool (n = 150 species) under low / high dispersal limitation. Dark and

693    light blue dots represent the environmental gradient ranging from -2 to +2. **(b)** We represent

694    the parameters of the SKRs ($R^2$, Y-intercept (alpha), slope of the SKRs (beta), distance to the

695    lower boundary) for each scenario using violin plots. We provide the mean overlap (Mo) among

696    the four scenarios. Different letters indicate significant differences between scenarios (overlap
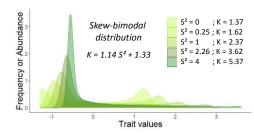
697    < 0.05; but NS for Not-Significant).

698     **FIGURES**

**(a)** *Trait distribution*



**(c)** *Example of a family of trait distributions*



**(b)** *Example of trait distributions*



**(d)** *The Skewness-Kurtosis Relationship (K = α + βS²)*



699

700     **Figure 1**

701

**(a)** Fixed Environment & Varying Species Pool

**(b)** Environmental gradient & Fixed Species Pool

702

703    **Figure 2**

704

705



706

**Figure 3**

708

**Figure 4**

709

710

711

712

**(a)** Skewness-Kurtosis space

**(b)** SKR parameters



Figure 5

713

714  **Figure 5**

715